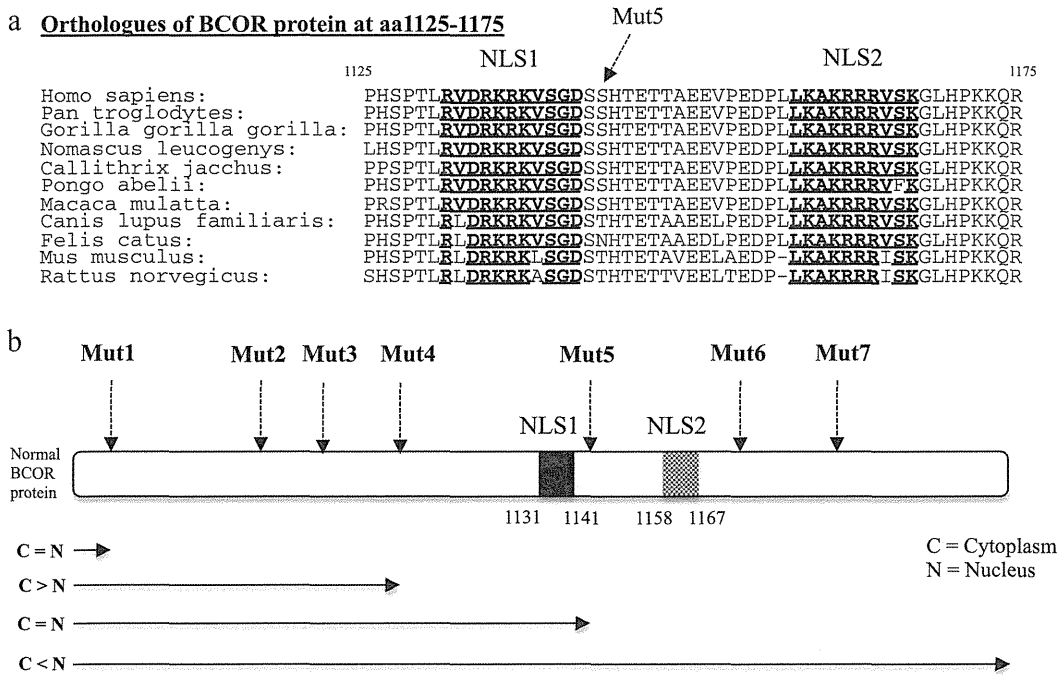

Fig. 3. The possible NLS sites. (a) The orthologs of BCOR protein at aa1125–1175. (b) The summary scheme of subcellular localization.

of BCOR protein and led to a diffuse cytoplasmic distribution. According to Fig. 5b and c, mutation of any of the KRRR amino acid residues at aa1161–1164 (NLS2Δ2–Δ5) in Mut6 increased protein diffusion in the cytoplasmic compartment of the transfected cells; however, the result was still showing that the mutant proteins expressed mainly in the nuclear compartment as shown in Fig. 5c, all ratios were above 1. As controls, mutations of amino acid residues flanking KRKR or KRRR did not affect the nuclear localization of Mut5 and Mut6.

3.5. The nuclear localization function of NLS2

NLS1 is not sufficient for perfect nuclear transport of the BCOR protein, as shown in the Mut5 immunofluorescence result. To determine whether NLS2 alone can function for complete transport of BCOR protein into the nucleus, we generated NLS1 critical region mutations in the Mut6 plasmid, L-NLS1Δ2, L-NLS1Δ3, and L-NLS1Δ4 (Fig. 6a). The results show that if NLS1 function is disrupted while NLS2 is intact, the protein can be transported into the nucleus and expressed mainly in the nucleus compartment (Fig. 6b and c).

4. Discussion

The nucleus, a specialized compartment for DNA separated from the rest of the cell by a membranous nuclear envelope in eukaryotic cells, establishes a connection between the nuclear transport machinery and the transcriptional apparatus. The cytoplasm and the nucleus intercommunicate via nuclear pore complexes, which are large transporters running through the nuclear membrane. Ions and small neutral proteins (<40kDa) pass through these complexes by passive diffusion. Therefore, the Mut1 protein (22.91kDa) can likely pass through the nuclear pore complex and be expressed in both the cytoplasm and nucleus.

Proteins involved in transcription and its regulation in response to distinct physiological conditions must be expressed in the nucleus to fulfill their functions [17]. Furthermore, BCOR is a transcriptional corepressor. Its main function occurs in the nucleus, so the transport of the BCOR protein after translation in the cytoplasm back into nucleus is very critical. Any protein that is not transported into the nucleus can be assumed to be non-functional. The best understood system for the transport of macromolecules between the cytoplasm and the nucleus is the classical nuclear import pathway. The first step of classical nuclear import occurs when importin-α discriminates between its cargo and other cellular proteins via the NLSs. According to the various *BCOR* isoforms, as well as our results for subcellular expression of mutant proteins and program analysis, the classical NLSs of the BCOR protein are located at two possible sites; RVDRKRKVSGD at aa1131–1141 (NLS1) and LKAKRRRVSK at aa1158–1167 (NLS2). Mutant proteins carrying neither NLS1 nor NLS2 are expressed mainly in cytoplasm. However, a mutant carrying only the NLS1 site was not sufficient for perfect transport of the protein into the nucleus. Complete transport of the protein was only detected when the protein contained both NLS1 and NLS2, or at least the intact NLS2. According to our results, the critical regions of NLS1 were the amino acid residues KRKR at aa1134–1137. The critical regions of NLS2 were more difficult to identify, but likely to be amino acid residues KRRR at aa1161–1164 that showed the lower fluorescence nucleus/cytoplasm ratio as shown in Fig. 5c. However, the protein expressions were mainly in the nucleus, cytoplasmic protein diffusion was detected more abundantly in NLS2Δ2–Δ5. A previous study showed that depending on the structure and characteristics of the mutant amino acid sequence, the binding affinity in the critical region in the NLS might be affected in a different manner [18]. Further studies are needed to clarify this mechanism.

To date, most of the reported *BCOR* mutations result in premature termination of the protein with deletion of the carboxy-terminal domain [1,3,6,13]. It was reported that truncated BCOR protein in affected patients displayed repressor effects equivalent to those of WT BCOR [3]. Therefore, we hypothesize the following: very small proteins (<40kDa) are too small to function and are degraded because of instability, even though they can

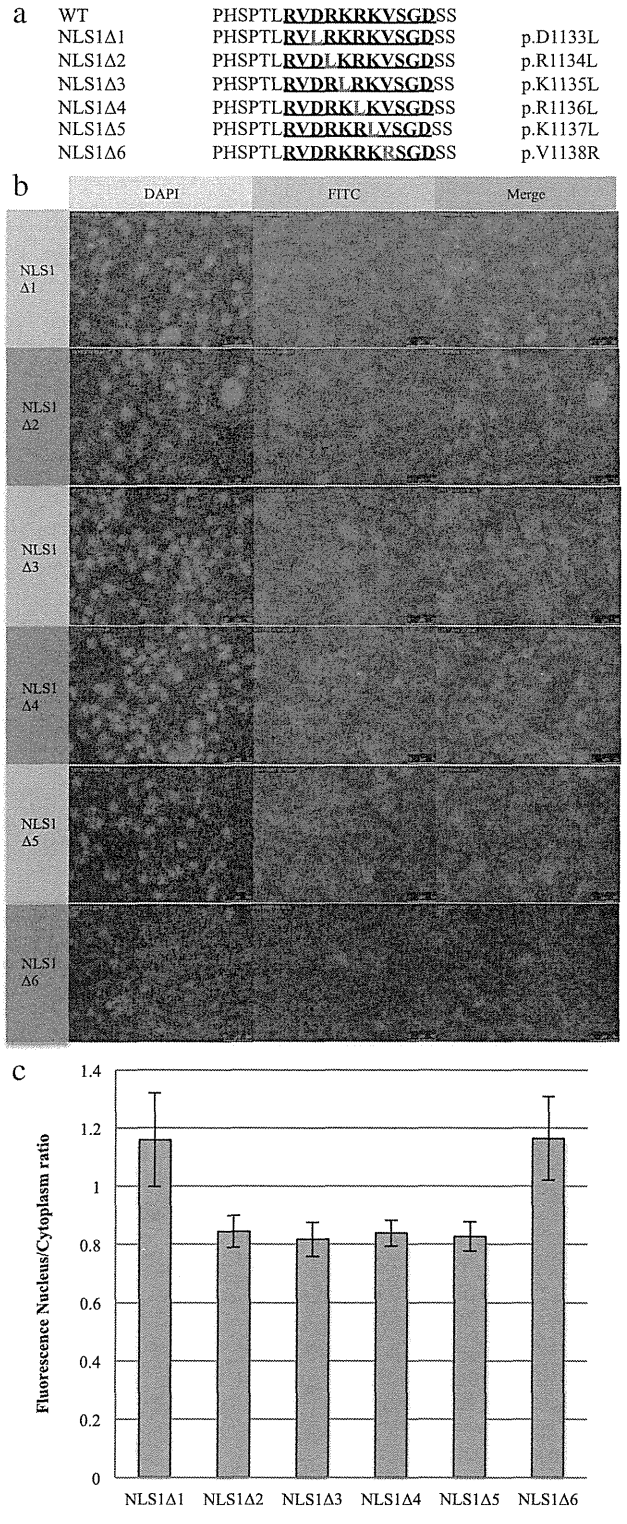

Fig. 4. Basic amino acid residues affected the NLS1. (a) Mut5 was used as the template to generate mutations inside the NLS1. (b) Mutation of any amino acid residue of KRKR at aa1134–1137 (NLS1Δ2–Δ5) severely disrupted the nuclear localization of the BCOR protein and led to a diffuse cytoplasmic distribution. As a control, mutation of amino acid residues flanking KRKR (NLS1Δ1 and Δ6) did not affect the nuclear localization of Mut5. (c) The fluorescence nucleus/cytoplasm ratio.

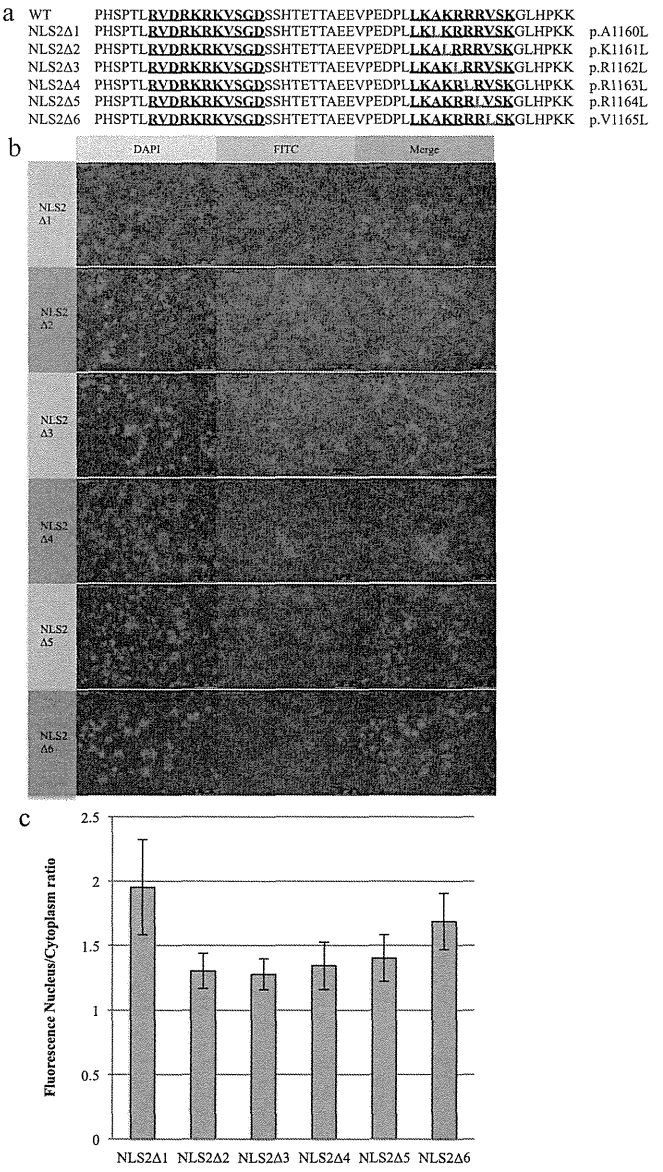

Fig. 5. Basic amino acid residues affected the NLS2. (a) Mut6 was used as the template to generate mutations inside the NLS2. (b) Although the mutation of any amino acid residue of KRRR at aa1161–1164 (NLS2Δ2–Δ5) led to increased protein diffusion into the cytoplasmic compartment of the transfected cells, the result was still showing that mutant protein expressions were mainly in the nuclear compartment. As a control, mutation of amino acid residues flanking KRRR (NLS2Δ1 and Δ6) did not affect the nuclear localization of Mut6. (c) The fluorescence nucleus/cytoplasm ratio.

travel through the nuclear pore and become expressed in both the nuclear and cytoplasmic compartments. Proteins that do not contain NLS1 or NLS2 would not be transported into the nucleus and could not function as transcriptional corepressors. Truncated proteins containing only NLS1 can partially be transported into the nucleus and might have partial function. Truncated proteins containing at least an intact NLS2 might be able to be normally transported into the nucleus and function; however, before translation into protein, mutant mRNA carrying a premature stop codon could be degraded by the non-sense-mediated mRNA decay mechanism, causing dramatically decreased mRNA levels and substantially decreased translation. It is likely that mutant cells would be haploinsufficient for WT BCOR protein, leading to typical OFCD conditions in BCOR-sensitive tissues.

Both NLS1 and NLS2 were possible sites as determined by program analysis and also were reported previously to have a certain nuclear transport function [15,16]. Multiple NLSs might afford redundancy in proteins that require nuclear import, each NLS

a

WT	PHSPTL**RVDRKRKVSGD**SSHTETTAEEVPEDPL**LKAKRRRVSK**GLHPKK	
L-NLS1Δ2	PHSPTL**RVDLKRKVSGD**SSHTETTAEEVPEDPL**LKAKRRRVSK**GLHPKK	p.R1134L
L-NLS1Δ3	PHSPTL**RVDRLRKVSGD**SSHTETTAEEVPEDPL**LKAKRRRVSK**GLHPKK	p.K1135L
L-NLS1Δ4	PHSPTL**RVDRKLKVSGD**SSHTETTAEEVPEDPL**LKAKRRRVSK**GLHPKK	p.R1136L

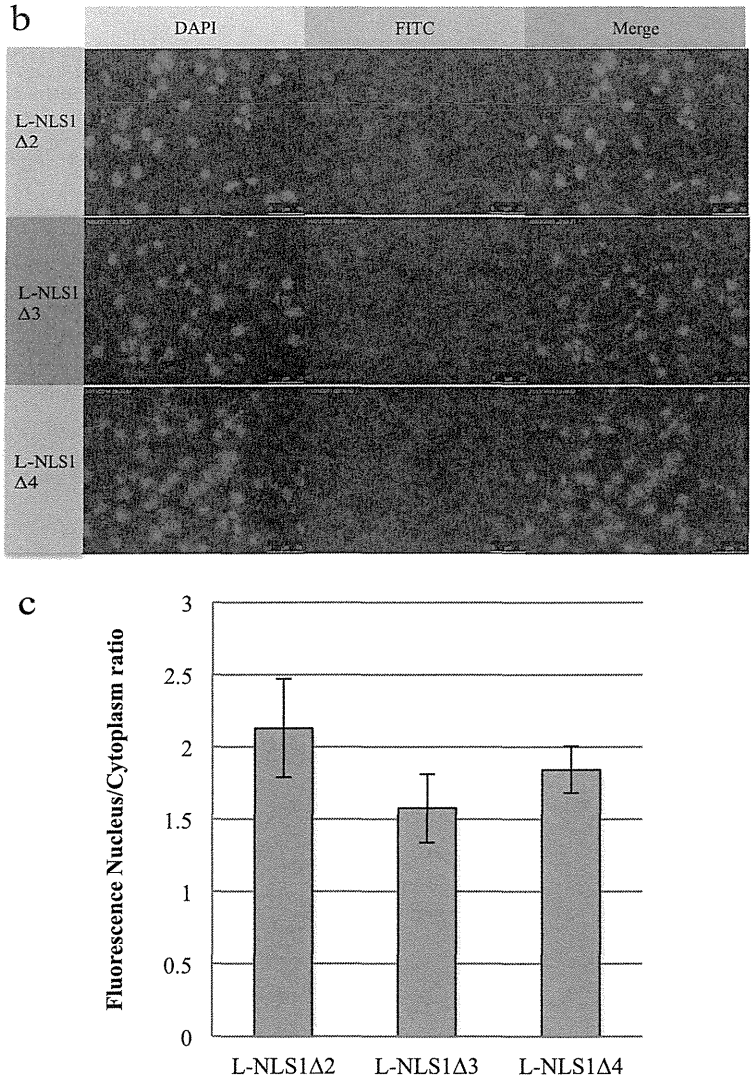

Fig. 6. The nuclear import function of independent NLS2 when NLS1 was disrupted. (a) Mut6 was used as the template to generate mutations inside the NLS1 (L-NLS1Δ2, L-NLS1Δ3, and L-NLS1Δ4). (b) The result showed that all mutant proteins were expressed mainly in the nucleus. (c) The fluorescence nucleus/cytoplasm ratio.

may use unique importin isoforms, or multiple NLSs may cooperate with one another and allow more efficient import. Possible variations of cooperation between multiple NLSs may allow fine control of nuclear import under various conditions [18]. In our study, NLS2 displayed a stronger nuclear import function than NLS1. Besides the amino acid sequences of the NLS, the three-dimensional conformation of the protein containing the NLS contributes to promote the specific binding of importin-α to the substrate [19]. Hence, the BCOR protein structure and the binding affinity of the NLSs to importin-α needs further study to clarify the relationship between NLS1 and NLS2.

To evaluate NLSs, deletion mutations within the gene of interest are typically generated and protein expression confirmed by immunofluorescence or immunoblotting. In our study, we did not perform the deletion method but instead generated mutations that were reported previously in different sites in the *BCOR* gene, to compare the clinical phenotypes and hopefully to identify a genotype-phenotype correlation. According to many previous studies, all mutations in the *BCOR* gene lead to similar phenotypes, but variations in severity were observed even in the same family carrying the same mutation. Therefore, the genotype-phenotype correlation is very complex and cannot explained by the mutation site alone. Other factors, such as mosaicism from X inactivation patterns and different sensitivities in the protective mechanisms in individuals might be involved in the severity of this syndrome.

In summary, although the genotype–phenotype correlation among the mutations could not be clearly explained, the classical NLSs were identified. Our study suggests that these two classical NLS sites are necessary for the perfect nuclear transport system of the BCOR protein. Further study will be needed to clarify the relationship between NLS1 and NLS2.

Acknowledgment

This work was supported by a Japan Society for the Promotion of Science Scientific Research (C) Grant (No. 25463167).

References

[1] Surapornsawasd, T., Ogawa, T., Tsuji, M. and Moriyama, K. (2014) Oculofaciocardiodental syndrome: novel BCOR mutations and expression in dental cells. J. Hum. Genet. 59, 314–320.

[2] Kantaputra, P.N. (2014) BCOR mutations and unstoppable root growth: a commentary on oculofaciocardiodental syndrome: novel BCOR mutations and expression in dental cells. J. Hum. Genet. 59, 297–299.

[3] Ng, D. et al. (2004) Oculofaciocardiodental and Lenz microphthalmia syndromes result from distinct classes of mutations in BCOR. Nat. Genet. 36, 411–416.

[4] Hilton, E. et al. (2009) BCOR analysis in patients with OFCD and Lenz microphthalmia syndromes, mental retardation with ocular anomalies, and cardiac laterality defects. Eur. J. Hum. Genet. 17, 1325–1335.

[5] Davoody, A., Chen, I.P., Nanda, R., Uribe, F. and Reichenberger, E.J. (2012) Oculofaciocardiodental syndrome: a rare case and review of the literature. Cleft Palate Craniofac. J. 49, e55–60.

[6] Oberoi, S., Winder, A.E., Johnston, J., Vargervik, K. and Slavotinek, A.M. (2005) Case reports of oculofaciocardiodental syndrome with unusual dental findings. Am. J. Med. Genet. A 136, 275–277.

[7] Hedera, P. and Gorski, J.L. (2003) Oculo-facio-cardio-dental syndrome: skewed X chromosome inactivation in mother and daughter suggest X-linked dominant Inheritance. Am. J. Med. Genet. A 123A, 261–266.

[8] Lozic, B., Ljubkovic, J., Panduric, D.G., Saltvig, I., Kutsche, K., Krzelj, V. and Zemunik, T. (2012) Oculo-facio-cardio-dental syndrome in three succeeding generations: genotypic data and phenotypic features. Braz. J. Med. Biol. Res. 45, 1315–1319.

[9] Huynh, K.D., Fischle, W., Verdin, E. and Bardwell, V.J. (2000) BCoR, a novel co-repressor involved in BCL-6 repression. Genes Dev. 14, 1810–1823.

[10] Gearhart, M.D., Corcoran, C.M., Wamstad, J.A. and Bardwell, V.J. (2006) Polycomb group and SCF ubiquitin ligases are found in a novel BCOR complex that is recruited to BCL6 targets. Mol. Cell. Biol. 26, 6880–6889.

[11] Srinivasan, R.S., de Erkenez, A.C. and Hemenway, C.S. (2003) The mixed lineage leukemia fusion partner AF9 binds specific isoforms of the BCL-6 corepressor. Oncogene 22, 3395–3406.

[12] Lange, A., Mills, R.E., Lange, C.J., Stewart, M., Devine, S.E. and Corbett, A.H. (2007) Classical nuclear localization signals: definition, function, and interaction with importin alpha. J. Biol. Chem. 282, 5101–5105.

[13] Horn, D. et al. (2005) Novel mutations in BCOR in three patients with oculo-facio-cardio-dental syndrome, but none in Lenz microphthalmia syndrome. Eur. J. Hum. Genet. 13, 563–569.

[14] Kosugi, S., Hasebe, M., Tomita, M. and Yanagawa, H. (2009) Systematic identification of cell cycle-dependent yeast nucleocytoplasmic shuttling proteins by prediction of composite motifs. Proc. Natl. Acad. Sci. U.S.A. 106, 10171–10176.

[15] Braem, C.V., Kas, K., Meyen, E., Debiec-Rychter, M., Van De Ven, W.J. and Voz, M.L. (2002) Identification of a karyopherin alpha 2 recognition site in PLAG1, which functions as a nuclear localization signal. J. Biol. Chem. 277, 19673–19678.

[16] Kaur, I. et al. (2011) Interleukin-4-inducing principle from Schistosoma mansoni eggs contains a functional C-terminal nuclear localization signal necessary for nuclear translocation in mammalian cells but not for its uptake. Infect. Immun. 79, 1779–1788.

[17] Turpin, P., Ossareh-Nazari, B. and Dargemont, C. (1999) Nuclear transport and transcriptional regulation. FEBS Lett. 452, 82–86.

[18] Prufer, K. and Boudreaux, J. (2007) Nuclear localization of liver X receptor alpha and beta is differentially regulated. J. Cell. Biochem. 100, 69–85.

[19] Freitas, N. and Cunha, C. (2009) Mechanisms and signals for the nuclear import of proteins. Curr. Genomics 10, 550–557.

Journal of Child Neurology
2015, Vol. 30(7) 932-936

DOI: 10.1177/0883073814541468
jcn.sagepub.com
SAGE

West Syndrome in a Patient With Schinzel-Giedion Syndrome

Fuyu Miyake, MD[1], Yukiko Kuroda, MD[1], Takuya Naruto, PhD[1], Ikuko Ohashi, MD[1], Kyoko Takano, MD[2], and Kenji Kurosawa, MD[1]

Abstract

Schinzel-Giedion syndrome is a rare recognizable malformation syndrome defined by characteristic facial features, profound developmental delay, severe growth failure, and multiple congenital anomalies. The causative gene of Schinzel-Giedion syndrome, *SETBP1*, has been identified, but limited cases have been confirmed by molecular analysis. We present a 9-month-old girl affected by West syndrome with Schinzel-Giedion syndrome. Congenital severe hydronephrosis, typical facial features, and multiple anomalies suggested a clinical diagnosis of Schinzel-Giedion syndrome. Hypsarrhythmia occurred at 7 months of age and was temporarily controlled by adrenocorticotropic hormone (ACTH) therapy during 5 weeks. *SETBP1* mutational analysis showed the presence of a recurrent mutation, p.Ile871Thr. The implications in management of Schinzel-Giedion syndrome are discussed.

Keywords

epilepsy, *SET binding protein 1 (SETBP1)*, adrenocorticotropic hormone (ACTH)

Received January 04, 2014. Received revised May 18, 2014. Accepted for publication June 01, 2014.

Schinzel-Giedion syndrome is a recognizable malformation syndrome characterized by midfacial retraction, hypertrichosis, congenital heart defects, urogenital malformations, predisposition to neoplasms, and multiple skeletal abnormalities. These skeletal abnormalities include a short and sclerotic skull base, short neck, talipes equinovarus, postaxial polydactyly, as well as profound developmental delay and epilepsy.[1,2] De novo dominant mutations of the SET binding protein 1 *(SETBP1)* gene have recently been described in individuals with Schinzel-Giedion syndrome.[3] Patients with Schinzel-Giedion syndrome often develop West syndrome and seizures that remain refractory to several anticonvulsive treatments.[4] We report a female genetically confirmed Schinzel-Giedion syndrome infant who had congenital bilateral hydronephrosis diagnosed prenatally, typical facial features, epilepsy, and multiple congenital anomalies. She developed West syndrome in the following months, and had partially effective adrenocorticotropic hormone (ACTH) therapy.

Case Report

The proposita was a female neonate born as the third child from healthy nonconsanguineous parents after an uneventful full term gestation. On prenatal ultrasonography, bilateral hydronephrosis was observed. Birth weight was 3450 g (+0.6 standard deviation) and head circumference 33.5 cm (0 standard deviation). Apgar scores were 7 at 1 minute and 8 at 5 minutes. Soon after birth, she developed respiratory distress because of thoracic hypoplasia and was treated by oxygen administration. Radiographic evaluation showed a sclerotic base, wide occipital synchondrosis, long clavicles, widening of distal femora/proximal humeri, and tibial bowing (Figure 1A). Dysmorphic features observed at birth included a widely open anterior fontanelle, upslanted palpebral fissure, hypertelorism, midface hypoplasia, and low-set dysplastic ears. She had a distinctive facial appearance with a wide mouth, retrognathia, and short nose with a low nasal bridge (Figure 1B). Ultrasonography of the abdomen showed bilateral hydronephrosis with severe dilation of both pelvicaliceal systems. Brain magnetic resonance imaging (MRI) showed cortical dysplasia and partial colpocephaly (Figure 1C). An echocardiogram showed a small ventricular septal defect. There were no remarkable findings on laboratory studies, including a thyroid function test. On day 2, she had apneic attacks and an electroencephalogram (EEG) showed spike-and-slow-wave complex patterns (Figure 2A). Following administration of phenobarbital, apneic attacks were

[1] Division of Medical Genetics, Kanagawa Children's Medical Center, Yokohama, Japan
[2] Division of Neurology, Kanagawa Children's Medical Center, Yokohama, Japan

Corresponding Author:
Kenji Kurosawa, MD, Division of Medical Genetics, Kanagawa Children's Medical Center, 2-138-4 Mutsukawa, Minami-ku, Yokohama, 232-8555, Japan.
Email: kkurosawa@kcmc.jp

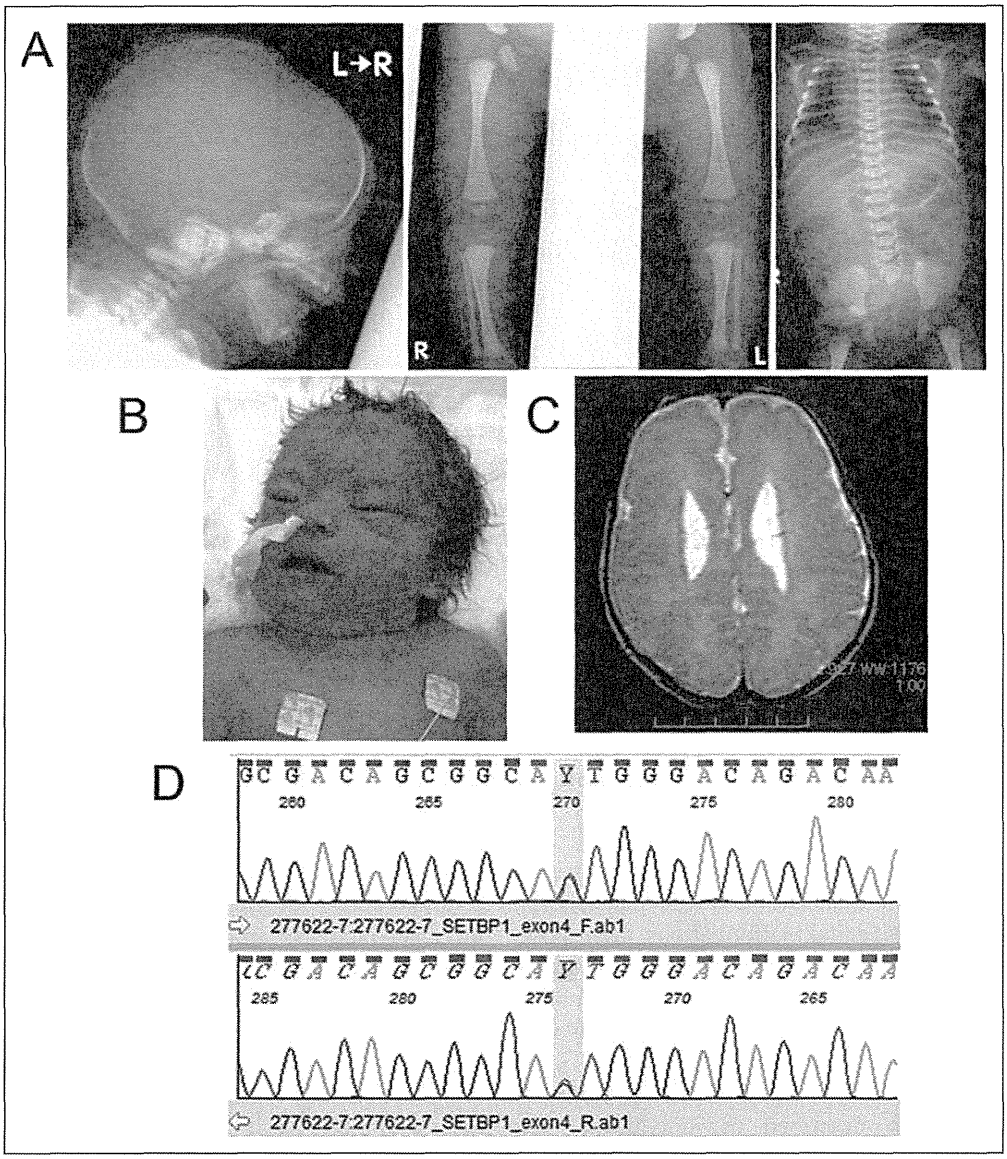

Figure 1. Clinical features and sequencing analysis of the patient. (A) Plain radiographs showing a sclerotic base, wide occipital synchondrosis, long clavicles, widening of distal femora/proximal humeri, and tibial bowing. (B) Photograph showing the patient on the first day of life. Note the widely open anterior fontanelle, upslanted palpebral fissure, hypertelorism, midface hypoplasia, and low-set dysplastic ears. (C) Magnetic resonance imaging (MRI) of the brain. Axial MRI T2 section at 7 months showing the ventricular enlargement and extraventricular enlargement, and delay of myelination. (D) Sequence of the *SETBP1* gene. The patient had a missense mutation, c.2612T>C (p.Ile871Thr) in the heterozygous state.

well controlled. At 23 days of age, she was discharged with oxygen and nasogastric tube feeding. She had no seizures and did not require oxygen or a nasogastric tube at 5 months (Figure 2B). At 7 months of age, she developed a series of spasms and myoclonus. EEG revealed large-amplitude (>600 μV) hypsarrhythmia (Figure 2C). Brain MRI showed ventricular and extraventricular enlargement, delay of myelination, and a thin corpus callosum. Phenobarbital had to be changed to valproic acid, vitamin B_6, and nitrazepam. Oral administration was not effective and then ACTH therapy was started. Seizures improved on the fourth day of treatment. After 2 weeks of treatment with ACTH, hypsarrhythmia patterns disappeared when she was awake, but remained during sleep on EEG (Figure 2D). On addition of ACTH administration on alternate days for 2 weeks, the EEG pattern was not improved. With ACTH treatment, no serious side effects were observed. The patient is currently 9 months old and her seizures relapsed 5 weeks after ACTH therapy started.

Characteristic clinical findings consistent with Schinzel-Giedion syndrome allowed us to perform direct sequencing analysis of exon 4 of the *SETBP1* gene. The primer sequences used were as described previously.[3] A recurrent de novo mutation, c.2612T>C (p.Ile871Thr), was detected in the heterozygous state (Figure 1D).

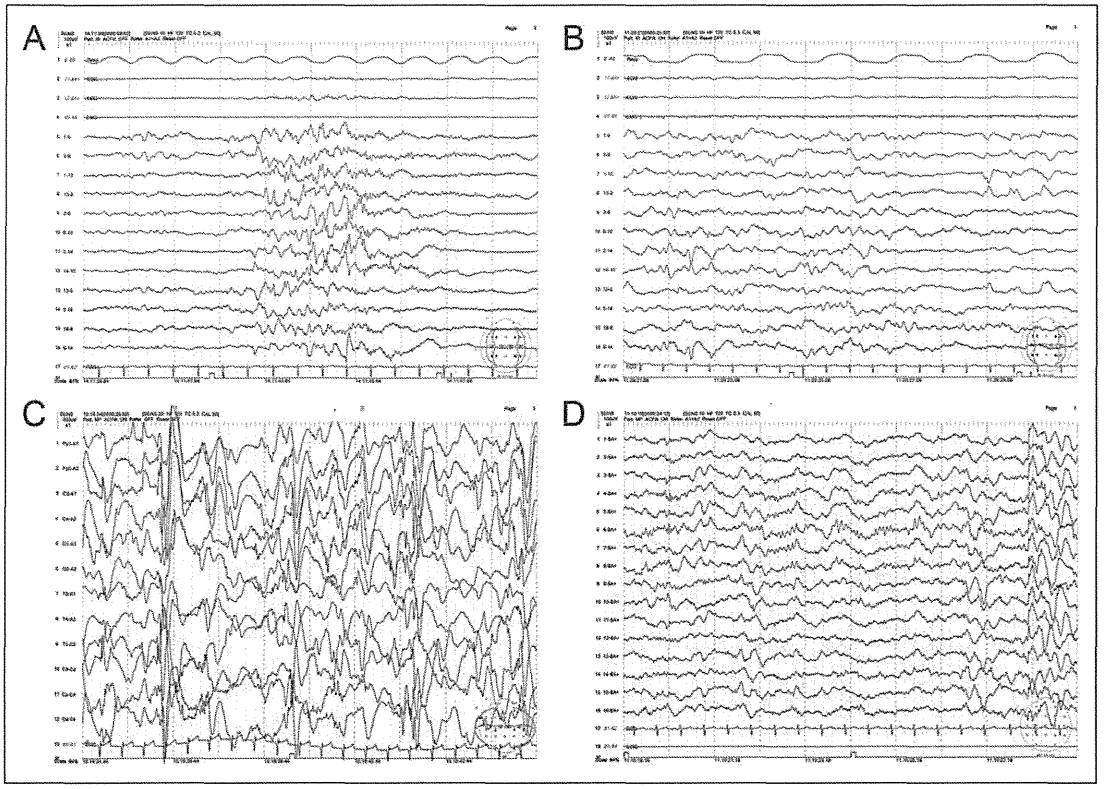

Figure 2. Electroencephalographic (EEG) tracing of the present case. (A) Day 2 after birth. (B) 23 days of age. (C) 7 months of age. Large-amplitude hypsarrhythmia was noted. (D) After 2 weeks of treatment with ACTH.

Discussion

Schinzel-Giedion syndrome is characterized by distinctive facial phenotype, including prominent forehead, midfacial retraction, and short and upturned nose. Typical skeletal abnormalities and hydronephrosis are major distinguishing features. Other supportive features include neuroepithelial tumors, hypertrichosis, and brain abnormalities. Severe developmental delay and poor prognosis is common to the previous reported cases.[2] This report describes neurologic features and the clinical course associated with West syndrome in a female infant with Schinzel-Giedion syndrome. She had bilateral hydronephrosis prenatally diagnosed, distinctive facial appearance, hirsutism, multiple skeletal abnormalities, and severe developmental delay. Brain MRI revealed ventriculomegaly and cortical dysplasia, and thin corpus callosum. These clinical findings were consistent with the cardinal features of Schinzel-Giedion syndrome.[5] She had a recurrent mutation, p.Ile871Thr, in *SETBP1*.

Central nervous system involvement appears as a prominent feature of Schinzel-Giedion syndrome with psychomotor deterioration and seizures.[4] Epilepsy is a common feature in patients with Schinzel-Giedion syndrome. EEG findings associated with Schinzel-Giedion syndrome include multifocal spikes or hypsarrhythmia. West syndrome has been reported in 25% of epileptic patients with Schinzel-Giedion syndrome.[4,6] Excluding our case, 15 of 16 patients reported as having *SETBP1* mutations had clinical seizures (Table 1).[3,7-9] In these patients with *SETBP1*, 2 had intractable seizures in several months,[8] and no patients developed West syndrome. In general, seizures in Schinzel-Giedion syndrome are extremely refractory to treatment with ACTH, antiepileptic drugs, and a ketogenic diet.[10] Antiepileptic drug therapy was effective in only 2 patients with seizures. One patient with neonatal tonic seizures was reported to be responsive to phenobarbital, but the long-term effect was unavailable in this case.[11] Another patient with partial seizures starting at the age of 2 months was controlled by combined therapy with phenobarbital and levetiracetam.[7] In our patient, phenobarbital was effective for neonatal apneic attacks with paroxysmal discharge. At 7 months of age, she developed a series of spasms. ACTH therapy was effective based on neurologic findings, but 5 weeks later, a series of spasms and myoclonus occurred. Unlike previous reports, our patient had a good response to ACTH therapy temporarily. These results suggested that selection of therapy for neurologic findings during the early stage has implications in the management of Schinzel-Giedion syndrome.

Gain-of-function or dominant negative mutation in *SETBP1*, a gene encoding SET-binding protein 1, is thought to be a causative mechanism in Schinzel-Giedion syndrome.[3] Further, several lines of recurrent evidence suggest that *SETBP1* plays a role in leukemogenesis.[12-14] Although *SETBP1* is a causative gene to be identified molecularly, the underlying pathophysiology in Schinzel-Giedion syndrome is poorly understood. The mutation identified in our patient, c.2612T>C (p. Ile871Thr), was

Table 1. Seizure Patterns and Therapy in Reported Schinzel-Giedion Syndrome Patients.

Clinical features	Present case	Ko et al, 2013[7]	Lestner et al, 2012[9]	Watanabe et al, 2013[6]	Grosso et al, 2003[4]
Genotype	I871T	G870S	I871T	NA	NA
Sex	F	M	M	M	M
Developmental delay	Severe	Severe	Severe	Severe	Severe
Brain MRI	Cortical dysplasia, partial colpocephaly, ventriculomegaly, myelination delay	Ventriculomegaly, myelination delay	Ventriculomegaly, polymicrogyria	Delayed myelination, cortical strophy, thin corpus callosum	Ventriculomegaly, cortical atrophy, thin corpus callosum
Age at onset of seizure (mo)	7	2	3	1	22
Seizure pattern	A series of spasms and myoclonus	Generalized tonic convulsions	Myoclonic seizures	Generalized tonic convulsions	Infantile spasm
Medications	Phenobarbital, valproic acid, vitamin B_6, nitrazepam, +ACTH	Phenobarbital, levetiracetam	Short course steroids, phenobarbitone, levetiracetam	Phenobarbital, valproic acid	ACTH, vigabatrin, valproic acid, benzodiazepine, topiramate, felbamate
Prognosis in seizure	Transient improved, relapsed	Well controlled at 10 mo	Partially responsive	No fundamental changes	Refractory

Abbreviations: MRI, magnetic resonance imaging; NA, not available.

previously reported in 6 of 15 patients with molecularly confirmed Schinzel-Giedion syndrome.[3,9] All 6 patients showed typical clinical features, including neurodevelopmental delay, and 1 patient had epilepsy. A definite genotype-phenotype correlation was not identified.

In conclusion, we report a patient with Schinzel-Giedion syndrome resulting from a *SETBP1* mutation who had bilateral hydronephrosis from the fetal period and typical clinical phenotypes, including neurodevelopmental delay and epilepsy. The epilepsy was intractable similar to previously reported cases. However, ACTH therapy for West syndrome in our patient was temporarily effective, which is different from previous reports. Although further investigation will be necessary to clarify the role of *SETBP1* mutations in Schinzel-Giedion syndrome, findings from our case suggest a therapeutic strategy for intractable epilepsy in Schinzel-Giedion syndrome.

Author Contributions

FM, YK, IO, and KT evaluated the patient. TN carried out the molecular genetic analysis. FM and YK drafted the manuscript and the other authors revised it critically for important intellectual content. KK performed critical review of the article.

Declaration of Conflicting Interests

The authors declared no potential conflicts of interest with respect to the research, authorship, and/or publication of this article.

Funding

The authors disclosed receipt of the following financial support for the research, authorship, and/or publication of this article: This research was supported in part by a Grant-in-aid from the Ministry of Health, Labour and Welfare, Japan.

Ethical Approval

Parental informed consent was obtained for publication of this article.

References

1. Schinzel A, Giedion A. A syndrome of midface retraction, multiple skull anomalies, clubfoot, and cardia and renal malformations in sibs. *Am J Med Genet*. 1978;1:361-375.
2. Lehman AM, McFadden D, Pugash D, et al. Schinzel-Giedion syndrome: Report of splenopancreatic fusion and proposed diagnostic criteria. *Am J Med Genet Part A*. 2008;146A:1299-1306.
3. Hoischen A, van Bon BW, Gilissen C, et al. De novo mutations of *SETBP1* cause Schinzel-Giedion syndrome. *Nat Genet*. 2010;42:483-485.
4. Grosso S, Pagano C, Cioni M, et al. Schinzel-Giedion syndrome: a further cause of West syndrome. *Brain Dev*. 2003;25:294-298.
5. Touge H, Fujinaga T, Okuda M, Aoshi H. Schinzel-Giedion syndrome. *Intern J Urol*. 2002;8:237-241.
6. Watanabe S, Murayama A, Haginoya K, et al. Schinzel-Giedion syndrome: a further cause of early myoclonic encephalopathy and vacuolating myelinopathy. *Brain Dev*. 2013;34:151-155.
7. Ko JM, Lim BC, Kim KJ, et al. Distinct neurological features in a patient with Schinzel-Giedion syndrome caused by a recurrent *SETBP1* mutation. *Childs Nerv Syst*. 2013;29:525-529.
8. Suphapeetiporn K, Srichomthong C, Shotelersuk V. *SETBP1* mutations in two Thai patients with Schinzel-Giedion syndrome. *Clin Genet*. 2011;79:391-393.
9. Lestner JM, Chong WK, Offiiah A, et al. Unusual neuroradiological features in Schinzel-Giedion syndrome: a novel case. *Clin Dysmorphol*. 2012;21:152-154.
10. Shah AM, Smith MF, Griffiths PD, Quarrell OW. Schinzel-Giedion syndrome: evidence for a neurogenerative process. *Am J Med Genet*. 1999;82:344-347.

11. McPherson E, Clemens M, Hoffner L, Surti U. Sacral tumors in Schinzel-Giedion syndrome. *Am J Med Genet*. 1998;79: 62-63.
12. Piazza R, Valletta S, Winkelmann N, et al. Recurrent *SETBP1* mutations in atypical chronic myeloid leukemia. *Nat Genet*. 2013;45:18-24.
13. Sakaguchi H, Okuno Y, Muramatsu H, et al. Exome sequencing identifies secondary mutations of *SETBP1* and *JAK3* in juvenile myelomonocytic leukemia. *Nat Genet*. 2013;45:937-941.
14. Makishima H, Yoshida K, Nguyen N, et al. Somatic *SETBP1* mutations in myeloid malignancies. *Nat Genet*. 2013;45:942-946.

CLINICAL REPORT

AMERICAN JOURNAL OF medical genetics PART A

Improved Growth Velocity of a Patient with Noonan-Like Syndrome with Loose Anagen Hair (NS/LAH) Without Growth Hormone Deficiency by Low-Dose Growth Hormone Therapy

Kei Takasawa,[1,2] Shigeru Takishima,[1] Chikako Morioka,[1] Masato Nishioka,[2] Hirofumi Ohashi,[3] Yoko Aoki,[4] Masayuki Shimohira,[2] Kenichi Kashimada,[1]* and Tomohiro Morio[1]

[1]Department of Pediatrics and Developmental Biology, Tokyo Medical and Dental University, Tokyo, Japan

[2]Department of Pediatrics, Kawaguchi Municipal Medical Center, Kawaguchi, Japan

[3]Division of Medical Genetics, Saitama Children's Medical Center, Saitama, Japan

[4]Department of Medical Genetics, Tohoku University School of Medicine, Sendai, Japan

Manuscript Received: 12 December 2014; Manuscript Accepted: 19 May 2015

Noonan-like syndrome with loose anagen hair (NS/LAH; OMIM 607721) is caused by a heterozygous c.4A>G mutation in *SHOC2*. Most cases exhibit both growth hormone deficiency (GHD) and growth hormone insensitivity (GHI) and thus require a high dose of growth hormone (GH) therapy (e.g., 35–40 μg/kg/day). We report on a genetically diagnosed NS/LAH patient manifesting severe short stature (−3.85 SDs) with low serum level of IGF1, 30 ng/ml. The peak levels of GH stimulation tests were within the normal range, and GHI was not observed in the IGF1 generation test. However, with low-dose GH therapy (25 μg/kg/day) for two years, IGF1 level and height were remarkably improved (IGF1: 117 ng/ml, height SDs: −2.20 SDs). Further, catch-up of motor development and improvement of the proportion of extending limbs to trunk were observed (the Developmental Quotient score increased from 68 to 98 points, and the relative sitting height ratio decreased from 0.62 to 0.57). Our results suggest that endocrinological causes for short stature are variable in NS/LAH and that GH therapy should be considered as a possible treatment for delayed development in NS/LAH. © 2015 Wiley Periodicals, Inc.

Key words: NS/LAH; GH therapy; SHOC2; GHD; GHI

How to Cite this Article:
Takasawa K, Takishima S, Morioka C, Nishioka M, Ohashi H, Aoki Y, Shimohira M, Kashimada K, Morio T. 2015. Improved growth velocity of a patient with Noonan-like syndrome with loose anagen hair (NS/LAH) without growth hormone deficiency by low-dose growth hormone therapy.
Am J Med Genet Part A 167A:2425–2429.

INTRODUCTION

Dysregulation of the RAS-MAPK signaling pathway has been recognized as the underlying cause of Noonan syndrome (NS) and related disorders [Aoki et al., 2008; Roberts et al., 2013], such as Costello syndrome, cardio-facio-cutaneous (CFC) syndrome, Noonan syndrome with multiple lentigines (NSML; previously referred to as LEOPARD syndrome), and neurofibromatosis type 1. Those disorders are collectively named RASopathies [Tidyman and Rauken, 2009; Tartaglia and Gelb, 2010]. Mazzanti syndrome (OMIM 607721), so-called Noonan-like syndrome with loose anagen hair (NS/LAH) is an NS-related disorder, having typical features of facial phenotype resembling NS, postnatal growth deficiency, congenital heart defects, mild intellectual disability, hypernasal or hoarse voice, darkly pigmented skin, and easily pluckable, sparse, slow growing hair [Mazzanti et al., 2003]. Recently, a missense mutation, c.4A>G (p.Ser2Gly) of Soc-2 Suppressor of Clear Homolog (*SHOC2*) was identified as a cause of NS/LAH [Cordeddu et al., 2009]. SHOC2 is a scaffold protein that links RAS to downstream signal transducers in the RAS/ERK MAP kinase signaling cascade.

The authors state that they have no conflict of interest.

*Correspondence to:
Kenichi Kashimada, M.D., Ph.D., Department of Pediatrics and Developmental Biology, Tokyo Medical and Dental University, 1-5-45 Yushima, Bunkyo-ku, Tokyo 113-8510, Japan.
E-mail: kkashimada.ped@tmd.ac.jp

Article first published online in Wiley Online Library (wileyonlinelibrary.com): 19 June 2015
DOI 10.1002/ajmg.a.37191

Short stature is one of the common features in NS and other RASopathies, and growth hormone (GH) therapy has been reported to improve height prognosis in NS [Ferreria et al., 2005; Dahlgren, 2009; Romano et al., 2009]. The severity of growth deficiency in RASopathies depends on the types of the disease. Especially, in NS/LAH, short stature is more severe than in other types of RASopathies [Malaquias et al., 2012]. Mild to moderate GH deficiency (GHD) and insensitivity to growth hormone (GHI) have been suggested as causes of short stature in NS/LAH patients [Cordeddu et al., 2009; Mazzanti et al., 2013]. To date, only two studies have examined the effects of GH treatment on NS/LAH [Capalbo et al., 2012a; Mazzanti et al., 2013]. In those reports, the effectiveness of GH therapy was limited because of partial GHI. As a result, the authors recommended a higher dose of GH for NS/LAH patients [Capalbo et al., 2012b; Mazzanti et al., 2013].

Here, we report on a case of an NS/LAH patient whose severe short stature (−3.85 SDs) was remarkably improved by low-dose GH therapy (25 μg/kg/day), suggesting that mechanisms other than GH resistance underlie the short stature of NS/LAH.

CLINICAL REPORT

The female patient was born at term (38 weeks and 5 days of gestation) after an uneventful pregnancy by spontaneous vaginal delivery from nonconsanguineous Japanese parents. Birth weight was 3.29 kg (+1.40 SDs), length was 47 cm (−0.78 SDs) and head circumference 34.5 cm (+1.00 SDs). She was admitted to our neonatal intensive care unit for 15 days for a transient feeding disorder. Pulmonary valve stenosis was identified at birth and follow-up. No history of malnutrition or infectious diseases was found.

She was referred to our department at the age of 3 years for short stature. Physical examination revealed macrocephaly, prominent forehead, hypertelorism, low-set and posterior rotated ears, hoarse voice, dark skin, loose anagen and sparse scalp hair, deep palmar, and plantar creases (Fig. 1). She had severe growth retardation: 12.4 kg (−0.82 SDs) in weight and 81.2 cm (−3.86 SDs) in height with impaired linear growth velocity (5.6 cm/year: −2.13 SDs; Fig. 2). The target height calculated from the parents' heights was 163.5 cm (+1.02 SDs). Relative sitting height, which is the ratio of sitting height to stature was 0.62. Bone age (TW2 Method) was delayed by 1.5 years, and the karyotype was 46, XX. Neurological evaluation revealed mild motor delay (a Developmental Quotient score of 68 points) with delayed walking (started at 2.5 years of age). Cerebral MRI showed no abnormalities.

Based on these findings, genes associated with RASopathies were screened and a c.4A>G, (p.Ser2Gly) mutation was identified in *SHOC2*, confirming the diagnosis of NS/LAH.

Serum IGF1 level (30 ng/ml) was low compared to age-matched reference levels of 40–227 ng/ml (Table I). However, the peak levels of GH following stimulation with insulin, arginine, GHRP-2, and GHRH (but not L-dopa) were in the normal range (Table II), suggesting that the patient does not have moderate–severe GHD. However, the IGF1 generation test (50 μg/kg/day of GH for 7 days) revealed a normal response, with IGF1 increasing from 30 to 70 ng/ml (Cut-off: ΔIGF1 < 15 ng/ml [Blum et al., 1994]).

The protocol of GH therapy for NS/LAH is not well established, and we started GH therapy with a lower dose, 25 μg/kg/day, the same as used for GHD. In contrast to previous case reports, the lower dose of GH therapy remarkably improved the linear growth of the patient, with her height reaching −2.20 SDs after 2 years of

FIG. 1. The patient at 3 years of age. A: Frontal view: macrocephaly, hypertelorism and flat nasal bridge. B: Side view: prominent forehead, low-set and posteriorly rotated ear, and sparse scalp hair (loose anagen hair).

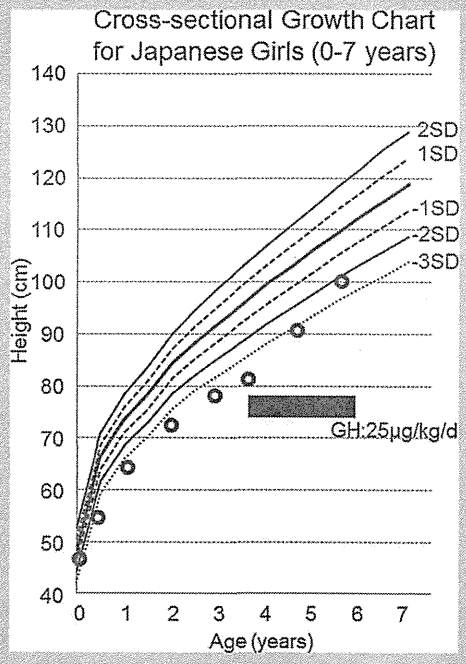

FIG. 2. Growth chart of the patient before and during GH therapy. GH therapy significantly improved growth velocity and the height of the patient improved from −3.86 to −2.20 SDs over a 2-year period.

TABLE I. IGF1 Levels of Patient Before Treatment

Age (months)	IGF1 value (ng/ml)	Age-matched reference level
27	8	32–213
37	20	40–227
44	34	40–227
46	30	40–227

TABLE II. Biochemical Evaluation of GH-IGF1 Axis

GH stimulation test		Basal GH value (ng/ml)	Peak GH value (ng/ml)	Cut-off
Insulin	(0.07 U/kg)	0.51	10.66	<6
Arginine	(0.5 g/kg)	0.50	9.40	<6
L-dopa	(10 mg/kg)	0.88	2.68	<6
GHRP-2	(2 μg/kg)	0.83	60.24	<16
GHRH	(1 μg/kg)	0.86	16.28	<9
IGF1 generation test*		**Before stimulation**	**After stimulation**	
IGF1 value (ng/ml)		30	70	

*rhGH 50 μg/kg/day × 7days.

treatment (Fig. 2). The age-matched linear growth velocity increased to +4.74 SDs. The serum levels of IGF1 increased to 117 ng/ml which is close to the average level of sex- and age-matched reference (56–252 ng/ml). Motor development and the extended limbs to trunk ratio also improved. The patient is presently five years old and has a DQ score of 98. Her relative sitting height ratio decreased to 0.57, which is in the normal range.

DISCUSSION

RASopathies are caused by mutations in genes that encode several proteins, including SHP2 (encoded by *PTPN11*), *SOS1*, *KRAS*, *HRAS*, *BRAF*, *RAF1*, and *MEK1/2*. These proteins positively contribute to RAS-MAPK signalling. The mutations impair complex autoinhibitory mechanisms resulting in abnormal activation of RAS-MAPK signalling [Aoki et al., 2008; Tartaglia et al., 2011]. The p.Ser2Gly amino acid substitution in *SHOC2* causes N-myristoylation resulting in aberrant constitutive targeting of the mutated protein to the plasma membrane and positively controlling RAF1 to increase ERK activation in a cell context-specific manner [Cordeddu et al., 2009].

One hypothesis is that the growth defects of RASopathies are due to IGF1 generation deficiency because RAS/ERK1/2 hyperactivation inhibits GH-induced IGF1 release [De Rocca Serra-Nédélec et al., 2012]. Most RASopathy cases show "mild" GHI including low serum level of IGF1 without GHD and with a blunted IGF1 response in an IGF1 generation test [Binder et al., 2005; Bertelloni et al., 2013].

In contrast to previously reported NS/LAH cases, the present case did not show impaired responses to GH stimulating tests or GH resistance. The present case revealed two clinical points about NS/LAH: (i) in some NS/LAH cases, severe GHD and GH resistance might not be a major cause for severe short stature in NS/LAH and (ii) GH therapy could assist neurological development of NS/LAH.

Although endocrinological data did not clearly indicate that the patient had moderate–severe GHD, the level of IGF1 was low, suggesting that endogenous GH was not sufficient for IGF1 synthesis. On the other hand, low-dose GH therapy effectively induced IGF1, resulting in a remarkable improvement in height velocity. Those findings might be simply explained by a milder phenotype of GHD, that is, despite of the normal responses of GH stimulation tests, the patient had mild GHD. GH stimulation tests have been suggested to have number of limitations including its reproducibility [Richmond and Rogol, 2008]. If the result of the GH stimulating tests is supposed to be true, a shift in higher threshold for IGF1 synthesis could be another possible explanation for the low IGF level in our case. However, this is a novel hypothesis just based on a single case study without molecular analysis, and further case studies are necessary to verify the second hypothesis.

Thus, our case suggests that endocrinological causes for short stature would be variable in NS/LAH, although NS/LAH is caused by a specific mutation in a specific gene. Unlike our case, most reported NS/LAH cases have low serum levels of IGF1 with a blunted IGF1 response to GH administration, so that they require a high dose GH (e.g., 35–45 μg/kg/day) [Capalbo et al., 2012b; Mazzanti et al., 2013] (Table III). Examination of additional

TABLE III. Effect of GH Therapy on NS/LAH

	Present case			Mazzant et al.				Capalbo et al.	
Sex	F	M	M	M	M	F	F	F	F
Birth length (cm)	47	48	49	47	49	46	48	45	48
Birth weight (g)	3,290	3,280	3,600	3,320	3,320	2,980	2,800	2,450	3,710
Target height (SDS)	1.02	−0.78	−0.80	−1.29	−0.40	0.72	−0.79	NA	NA
GHD	−	+	+	+	+	+	+	−	+
GV before GH therapy									
SDS	−2.10	−2.25	−2.85	−1.75	−2.03	−2.34	−1.10	NA	NA
cm/year	5.6	NA	NA	NA	NA	NA	NA	3	NA
Age at GH-start (years)	3.7	3.1	3.0	7.5	4.4	2.6	9.4	7	11
Height at GH-start (SDS)	−3.86	−2.36	−2.82	−3.46	−2.92	−4.76	−3.93	−5.70	−3.21
IGF1 at GH-start									
SDS	−2.26	−2.62	−1.97	NA	−2.30	−3.37	−3.93	−2.46	NA
ng/ml (reference level)	30 (40–227)	NA	NA	NA	NA	NA	NA	27 (60–350)	NA
Dose of GH (μg/kg/day)	25	35	35	35	35	35	35	45	40
IGF1 after GH therapy									
SDS	−0.76	−0.70	−0.25	NA	0.25	−0.7	NA	−2.58	NA
ng/ml (reference level)	117 (56–252)	NA	NA	NA	NA	NA	NA	93.5 (180–780)	NA
Duration GH therapy (years)	2	14.8	1	NA	1	11.3	1	6	6
GV 1st year GH therapy (SDS)	4.90	3.12	1.65	NA	3.50	4.12	2.79	NA NA	
Height after GH therapy (SDS)	−2.20	−2.32	NA	NA	NA	−2.47	NA	−5	<−2

GHD, growth Hhormone deficiency; GV, growth velocity; NA, not available.

GH-treated NS/LAH cases is needed to identify the precise mechanisms of growth retardation in NS/LAH and to determine the optimal dose of GH therapy according to each case.

GH therapy from early childhood could improve motor development of NS/LAH patients. Extension of the limb lengths and strengthened muscles tonus were observed after 2 years of GH therapy, following improvement of gross motor skills. Because IGF1 appears to play a major role in the regulation of skeletal muscle tonus [Schiaffino and Mammucari, 2011], the dramatic increase in the level of IGF1 by GH therapy in the present study might have contributed to the improvement of motor development. Our results suggest that that the decision to use GH therapy in NS/LAH patients should be based not only on short stature but also on developmental delay.

In conclusion, our results suggest that the effects of GH therapy in NS/LAH are various, and low-dose GH therapy might be effective for short stature and motor delay in NS/LAH patients. Further studies are needed to clarify the clinical and molecular details of the growth retardation in NS/LAH.

REFERENCES

Aoki Y, Niihori T, Narumi Y, Kure S, Matsubara Y. 2008. The RAS/MAPK syndromes: Novel roles of the RAS pathway in human genetic disorders. Hum Mutat 29:992–1006.

Bertelloni S, Baroncelli GI, Dati E, Ghione S, Baldinotti F, Toschi B, Simi P. 2013. IGF-I generation test in prepubertal children with Noonan syndrome due to mutations in the PTPN11 gene. Hormones (Athens) 12:86–92.

Binder G, Neuer K, Ranke MB, Wittekindt NE. 2005. PTPN11 mutations are associated with mild growth hormone resistance in individuals with Noonan syndrome. J Clin Endocrinol Metab 90:5377–5381.

Blum WF, Cotterill AM, Postel-Vinay MC, Ranke MB, Savage MO, Wilton P. 1994. Improvement of diagnostic criteria in growth hormone insensitivity syndrome: Solutions and pitfalls. Pharmacia study group on insulin-like growth factor i treatment in growth hormone insensitivity syndromes. Acta Paediatr Suppl 399:117–124.

Capalbo D, Melis D, De Martino L, Palamaro L, Riccomagno S, Bona G, Cordeddu V, Pignata C, Salerno M. 2012a. Noonan-like syndrome with loose anagen hair associated with growth hormone insensitivity and atypical neurological manifestation. Am J Med Genet Part A 158A:856–860.

Capalbo D, Scala MG, Melin D, Minopoli G, Improda N, Palamaro L, Pignata C, Salerno M. 2012b. Heterogeneity in two patients with Noonan like Syndrome associated with the same SHOC2 mutation. Ital J Pediatr 38:48.

Cordeddu V, DiSchiavi E, Pennacchio LA, Ma'ayan A, Sarkozy A, Fodale V, Cecchetti S, Cardinale A, Martin J, Schackwitz W, Lipzen A, Zampino G, Mazzanti L, Digilio MG, Martinelli S, Flex E, Lepri F, Bartholdi D, Kutsche K, Ferrero GB, Anichini C, Selicorni A, Rossi C, Tenconi R, Zenker M, Merlo D, Dallapiccola B, Iyengar R, Bazzicalupo P, Gelb BD, Tartaglia M. 2009. Mutation of SHOC2 promotes aberrant protein N-myristoylation and causes Noonan-like syndrome with loose anagen hair. Nat Genet 41:1022–1026.

Dahlgren J. 2009. GH therapy in Noonan syndrome. Horm Res 72:46–48.

De Rocca Serra-Nédélec A, Edouard T, Tréguer K, Tajan M, Araki T, Dance M, Mus M, Montagner A, Tauber M, Salles JP, Valet P, Neel BG, Raynal P, Yart A. 2012. Noonan syndrome-causing SHP2 mutants inhibit insulin- like growth factor 1 release via growth hormone-induced ERK hyperactivation, which contributes to short stature. PNAS 109:4257–4262.

Ferreria LV, Souza ALS, Arnhold IJP, Mendoca BB, Jorge AAL. 2005. PTP11 (Protein tyrosine phosphatise non receptor type 11) mutations and response to growth hormone therapy in children with Noonan Syndrome. J Clin Endocrinology Metab 90:5156–5160.

Malaquias AC, Brasil AS, Pereira AC, Arnhold IJP, Mendonca BB, Bertola DR, Jorge AAL. 2012. Growth standards of patients with Noonan and Noonan-like syndromes with mutations in the RAS/MAPK pathway. Am J Med Genet Part A 158A:2700–2706.

Mazzanti L, Cacciari E, Cicognani A, Bergamascgi R, Scarano E, Forabosco A. 2003. Noonan-like syndrome with loose anagen hair: A new syndrome? Am J Med Genet A 118A:279–286.

Mazzanti L, Tamburrino F, Scarano E, Perri A, Vestrucci B, Guidetti M, Rossi C, Tartaglia M. 2013. GH Therapy and first final height data in Noonan-like syndrome with loose anagen hair (Mazzanti syndrome). Am J Med Genet A 161A:2756–2761.

Richmond EJ, Rogol AD. 2008. Growth hormone deficiency in children. Pituitary 11:115–120.

Roberts AE, Allanson JE, Tartaglia M, Gelb BD. 2013. Noonan syndrome. Lancet 381:333–342.

Romano AA, Dana K, Bakker B, Davis DA, Hunold JJ, Jacobs J, Lippe B. 2009. Growth response, near-adult height, and patterns of growth and puberty in patients with Noonan syndrome treated with growth hormone. J Clin Endocrinol Metab 94:2338–2344.

Schiaffino S, Mammucari C. 2011. Regulation of skeletal muscle growth by the IGF1-Akt/PKB pathway: Insights from genetic models. Skelet Muscle 1:4.

Tartaglia M, Gelb BD. 2010. Disorders of dis regulated signal traffic through the RAS-MAPK pathway: Phenotypic spectrum and molecular mechanism. Ann NY Acad Sci 1214:99–121.

Tartaglia M, Gelb BD, Zenker M. 2011. Noonan syndrome and clinically related disorders. Best Pract Res Clin Endocrinol Metab 25:161–179.

Tidyman WE, Rauken KA. 2009. The RASopathies: Developmental syndromes of Ras/MAPK pathway dysregulations. Currently Opin Genet Dev 19:230–236.

PEDIATRICS INTERNATIONAL Official Journal of the Japan Pediatric Society

Pediatrics International (2016) **58**, 88–99 doi: 10.1111/ped.12878

Review Article

CHST14/D4ST1 deficiency: New form of Ehlers–Danlos syndrome

Tomoki Kosho

Department of Medical Genetics, Shinshu University School of Medicine, Matsumoto, Japan

Abstract Carbohydrate sulfotransferase 14/dermatan 4-*O*-sulfotransferase-1 (CHST14/D4ST1) deficiency represents a specific form of Ehlers–Danlos syndrome (EDS) caused by recessive loss-of-function mutations in *CHST14*. The disorder has been independently termed "adducted thumb–clubfoot syndrome", "EDS, Kosho type", and "EDS, musculocontractural type". To date, 31 affected patients from 21 families have been described. Clinically, CHST14/D4ST1 deficiency is characterized by multiple congenital malformations (craniofacial features including large fontanelle, hypertelorism, short and downslanting palpebral fissures, blue sclerae, short nose with hypoplastic columella, low-set and rotated ears, high palate, long philtrum, thin upper lip vermilion, small mouth, and micro-retrognathia; multiple congenital contractures including adduction–flexion contractures and talipes equinovarus as well as other visceral or ophthalmological malformations) and progressive multisystem fragility-related complications (skin hyperextensibility, bruisability, and fragility with atrophic scars; recurrent dislocations; progressive talipes or spinal deformities; pneumothorax or pneumohemothorax; large subcutaneous hematomas; and diverticular perforation). Etiologically, multisystem fragility is presumably caused by impaired assembly of collagen fibrils resulting from loss of dermatan sulfate (DS) in the decorin glycosaminoglycan side chain that promotes electrostatic binding between collagen fibrils. This is the first reported human disorder that specifically affects biosynthesis of DS. Its clinical characteristics indicate that CHST14/D4ST1 and, more fundamentally, DS, play a critical role in fetal development and maintenance of connective tissues in multiple organs. Considering that patients with CHST14/D4ST1 deficiency develop progressive multisystem fragility-related manifestations, establishment of a comprehensive and detailed natural history and health-care guidelines as well as further elucidation of the pathophysiology in view of future etiology-based therapy are crucial.

Key words carbohydrate sulfotransferase 14, dermatan 4-*O*-sulfotransferase-1, dermatan sulfate, Ehlers–Danlos syndrome.

Ehlers–Danlos syndrome (EDS) is a heterogeneous group of heritable connective tissue disorders, the hallmarks of which are skin hyperextensibility, joint hypermobility, and tissue fragility involving the skin, ligaments, joints, blood vessels, and internal organs.[1] Dominant negative effects or haploinsufficiency of mutant procollagen α-chain genes or deficiency of collagen-processing enzymes have been identified as the basis for various types of EDS.[2] The present nosology for EDS was established at a nomenclature conference held at Villefranche-sur-Mer, France in 1997. EDS was classified into six major types: classical type (MIM#130000), hypermobility type (MIM%130020), vascular type (MIM 130050), kyphoscoliosis type (MIM#225400), arthrochalasia type (MIM#130060), and dermatosparaxis type (MIM#225410) (Table 1).[3] Additional forms of EDS have also been identified in association with molecular and biochemical abnormalities (Table 1).[4] This review article provides a brief history and describes the clinical features and molecular, glycobiological, and pathological characteristics of a recently delineated form of EDS caused by carbohydrate sulfotransferase 14/dermatan 4-*O*-sulfotransferase-1 (CHST14/D4ST1) deficiency.

Correspondence: Tomoki Kosho, MD, Department of Medical Genetics, Shinshu University School of Medicine, 3-1-1 Asahi, Matsumoto 390-8621, Japan. Email: ktomoki@shinshu-u.ac.jp

Received 6 September 2015; revised 30 October 2015; accepted 1 December 2015.

History

Ehlers–Danlos syndrome caused by CHST14/D4ST1 deficiency has been identified as three independently reported conditions: a rare type of arthrogryposis syndrome, "adducted thumb–clubfoot syndrome";[5] a specific type of EDS, "EDS, Kosho type";[6,7] and a subset of kyphoscoliosis-type EDS without lysyl hydroxylase deficiency, "musculocontractural EDS",[8] all of which are now concluded to be a single clinical entity.

Adducted thumb–clubfoot syndrome

Dündar *et al.* wrote the original report on adducted thumb–clubfoot syndrome in 1997.[9] Two cousins, a 3.5-year-old boy and a 1.5-year-old girl from a consanguineous Turkish family, were described as both having moderate to severe psychomotor developmental delay, ocular anterior chamber abnormalities, characteristic facial features, generalized joint laxity, arachnodactyly, camptodactyly, and distal arthrogryposis with adducted thumbs and clubfeet. The authors named this condition "adducted thumb–clubfoot syndrome". They subsequently reported a similar case involving a 3-month-old boy from a consanguineous Turkish family with three other affected siblings who died of an unknown etiology in early infancy.[10] The authors also suggested that two brothers from a Japanese consanguineous family aged 1 year 10 months and 7 months, respectively had adducted thumb–clubfoot syndrome.[11] Both brothers had multiple distal arthrogryposis, characteristic facial features, cleft

Table 1 Classification of Ehlers–Danlos syndrome (EDS)

	Prevalence[†]	Inheritance	Causative gene
Major types			
Classical type	1/20 000	AD	*COL5A1*, *COL5A2*
Hypermobility type	1/5000–20 000	AD	*TNXB*[‡]
Vascular type	1/50 000–250 000	AD	*COL3A1*
Kyphoscoliosis type	1/100 000	AR	*PLOD*
Arthrochalasia type	49	AD	*COL1A1*[§], *COL1A2*[§]
Dermatosparaxis type	8	AR	*ADAMTS-2*
Other forms			
Brittle cornea syndrome	11	AR	*ZNF469*
EDS-like syndrome due to tenascin-XB deficiency	10	AR	*TNXB*
Progeroid form	3	AR	*B4GALT7*, *B3GALT6*
Cardiac valvular form	4	AR	*COL1A2*
Spondylocheirodysplastic EDS	8	AR	*SLC39A13*
EDS caused by CHST14/D4ST1 deficiency	31	AR	*CHST14*

[†]n, sum of previously reported patients; [‡]in a small subset of cases; [§]splice-site mutations. AD, autosomal dominant; *ADAMTS2*; procollagen I N-proteinase; AR, autosomal recessive; *B3GALT6*, UDP-Gal, β-Gal β-1,3-galactosyltransferase, polypeptide 6; *B4GALT7*, xylosylprotein 4-β-galactosyltransferase, polypeptide 7; *CHST14*, carbohydrate sulfotransferase 14; *COL1A1* or *COL1A2*, α1(I) or α2(I) procollagen; *COL3A1*, α1(III) procollagen; *COL5A1* or *COL5A2*, α1(V) or α2(V) procollagen; D4ST1, dermatan 4-*O*-sulfotransferase-1; *FKBP14*, FK506-binding protein 14; *PLOD*, lysyl hydroxylase; *SLC39A13*, a membrane-bound zinc transporter; *TNXB*, tenascin-X; *ZNF469*, zinc finger protein 469.

palate, short stature, hydronephrosis, cryptorchidism, and normal intelligence. Additionally, Janecke *et al.* described two brothers with adducted thumb–clubfoot syndrome from a consanguineous Austrian family.[12] The authors concluded that these conditions represent a new type of arthrogryposis with central nervous system involvement, congenital heart defects, urogenital defects, myopathy, connective tissue involvement (generalized joint laxity), and normal or subnormal intellectual development. In 2009, Dündar *et al.* stated that adducted thumb–clubfoot syndrome was caused by loss-of-function mutations in *CHST14* encoding CHST14/D4ST1, through homozygosity mapping using samples from previous consanguineous families.[5] Glycobiological abnormalities were also demonstrated by Dündar *et al.*[5] They described patients with follow-up clinical findings of generalized joint laxity, delayed wound healing, ecchymoses, hematomas, and osteopenia/osteoporosis; the authors therefore categorized adducted thumb–clubfoot syndrome as a generalized connective tissue disorder.

EDS, Kosho type

In 2000, we encountered the first patient with a specific type of EDS, and a second with parental consanguinity was encountered in 2003. Both patients were Japanese girls with characteristic craniofacial features, skeletal features (multiple congenital contractures, marfanoid habitus, pectus excavatum, generalized joint laxity, recurrent dislocations, progressive talipes, and spinal deformity), cutaneous features (hyperextensibility, bruisability, and fragility with atrophic scars), recurrent large subcutaneous hematomas, and hypotonia with mild motor developmental delay.[13] These features strikingly overlapped those of Pakistani siblings classified as having a rare variant of kyphoscoliosis-type EDS with normal lysyl hydroxylase activity (EDS type VIB).[14] Therefore, we proposed that our two patients had a clinically recognizable subgroup of EDS, tentatively classified as EDS type VIB.[13] We subsequently encountered four additional unrelated Japanese patients with similar features, including a male patient with parental consanguinity and another male patient reported by Yasui *et al.*[15] We described the detailed clinical information of these four patients as well as the follow-up information of the two previously reported patients, and concluded that they had a new clinically recognized form of EDS with distinct craniofacial features, multiple congenital contractures, and multisystem fragility-related manifestations.[6] The condition we proposed has been registered as EDS, Kosho type in the London Dysmorphology Database (http://www.lmdatabases.com/index.html) and in POSSUM (http://www.possum.net.au/). A collaborative study by Miyake *et al.* identified *CHST14* as the causal gene for this condition through homozygosity mapping using the two consanguineous families in 2009.[7] Miyake *et al.* also demonstrated glycobiological abnormalities.[7]

Musculocontractural EDS

Malfait *et al.* identified mutations in *CHST14* through homozygosity mapping in two Turkish sisters and an Indian girl, both with parental consanguinity.[8] The patients shared characteristic craniofacial features, joint contractures, and wrinkled palms in addition to common features of kyphoscoliosis-type EDS, including kyphoscoliosis; joint hypermobility; muscular hypotonia; hyperextensible, thin, and bruisable skin with atrophic scarring; and ocular complications.[8] The authors concluded that these patients and those diagnosed with adducted thumb–clubfoot syndrome or EDS, Kosho type had a single clinical condition, which they termed "musculocontractural EDS".[8]

Clinical features

To date, 31 patients with recessive *CHST14* mutations (15 female, 16 male) from 21 families have been described (Table 2).[5,6,8–13,15–20]

Table 2 Reported patients with EDS caused by CHST14/D4ST1 deficiency

Patient	Family	Origin	*CHST14* mutations	Sex	Age†	Reference
1	1	Turkish	V49X homo	F	3.5 years	Dündar *et al.*[5,9]
2				M	1.5 years	
3				F	6 years	
4	2	Japanese	Y293C homo	M	4 years	Sonoda and Kouno[11]
5				M	7 months	
6	3	Austrian	R213P homo	M	0 days‡	Janecke *et al.*[12]
7				M	12 months	
8	4	Turkish	[R135G;L137Q] homo		1–4 months‡	Dündar *et al.*[10]
9				M	1–4 months‡	
10				M	1–4 months‡	
11				M	3 months	
12	5	Japanese	P281L/Y293C	F	11 years	Kosho *et al.*[6,13]
13	6	Japanese	P281L homo	F	14 years	Kosho *et al.*[6,13]
14	7	Japanese	P281L homo	M	32 years	Kosho *et al.*[6]
15	8	Japanese	K69X/P281L	M	32 years	Kosho *et al.*;[6] Yasui *et al.*[15]
16	9	Japanese	P281L/C289S	F	20 years	Kosho *et al.*[6]
17	10	Japanese	P281L/Y293C	F	4 years	Kosho *et al.*[6]
18	11	Turkish	V49X homo	F	22 years	Malfait *et al.*[8]
19				F	21 years	
20	12	Indian	E334Gfs*107 homo	F	12 years	Malfait *et al.*[8]
21	13	Japanese	P281L/Y293C	M	2 years	Shimizu *et al.*[16]
22	14	Japanese	F209S/P281L	M	6 years	Shimizu *et al.*[16]
23	15	Dutch	V49X homo	F	20 years	Voermans *et al.*[18]
24	16	Afghani	R274P homo	F	11 years	Mendoza-Lodondo *et al.*[17]
25				F	0 years	
26	17	Miccosukee	G228Lfs*13 homo	F	16 years	Winters *et al.*[19]
27	18	Asian	M280L homo	M	20 years	Syx *et al.*[20]
28	19	Curacao	Q133Rfs*14 homo	F	36 years	Syx *et al.*[20]
29	20	Moroccan	R29Gfs*113 homo	M	6 years	Syx *et al.*[20]
30	21	Asian	R218S homo	M	23 years	Syx *et al.*[20]
31				M	18 years	Syx *et al.*[20]

†At initial publication; ‡dead at time of initial publication. /, compound heterozygous mutation; D4ST1, dermatan 4-*O*-sulfotransferase-1; EDS, Ehlers–Danlos syndrome; homo, homozygous mutation.

Craniofacial features

Characteristic craniofacial features include a large fontanelle, hypertelorism, short and downslanting palpebral fissures, blue sclerae, short nose with hypoplastic columella, low-set and rotated ears, high palate, long philtrum, thin upper lip vermilion, small mouth, and micro-retrognathia at birth to early childhood (Fig. 1a,b,d,e,g,i–l). Slender and asymmetrical facial shape with protruding jaw are evident from adolescence (Fig. 1c,f,h).

Skeletal features

Multiple congenital contractures are cardinal features and typically include adduction–flexion contractures of the thumbs and talipes equinovarus (Fig. 2a,b,e,h,j). Finger shapes are characteristically described as "tapering", "slender", or "cylindrical" (Fig. 2c,d,f,g). Talipes deformities (planus, valgus, or severer; Fig. 2i,k) and spinal deformities (decreased physiological curvature, scoliosis, or kyphoscoliosis; Fig. 2r,s) are evident and frequently progressive. Marfanoid habitus, recurrent joint dislocations, and pectus deformities (flat and thin, excavatum, or carinatum) are also noted.

Cutaneous features

Skin hyperextensibility (from childhood; Fig. 2l,m), redundancy (from adolescence; Fig. 2n), bruisability, and fragility with atrophic scars (Fig. 2o) are generally observed. Acrogeria-like fine palmar creases or wrinkles are characteristic and become evident with aging (Fig. 2d,f,g). Hyperalgesia to pressure has been suggested in several patients because they disliked being hugged in infancy or disliked blood pressure measurement in the upper arms. Recurrent subcutaneous infection with fistula formation has also been observed.

Cardiovascular features

Recurrent large subcutaneous hematomas (skull, extremities, or hips) are a serious complication that can, even after minor trauma, progress acutely and massively to hemorrhagic shock requiring intensive treatment (hospital admission, blood transfusion, or surgical drainage; Fig. 2p,q). Intranasal 1-desamino-8-D-arginine vasopressin (DDAVP) treatment after trauma effectively prevented large subcutaneous hematomas in two patients.[6,13,15] Congenital heart defects, typically atrial septal defects, were detected in six patients. Valve abnormalities and/or aortic root dilatation were also detected in several patients. Infectious endocarditis requiring surgery occurred in one patient and was associated with regurgitation of the aortic valve or mitral valve.

Pulmonary features

Pneumothorax or pneumohemothorax occurred in three adult patients, who were treated with chest tube drainage.[6]

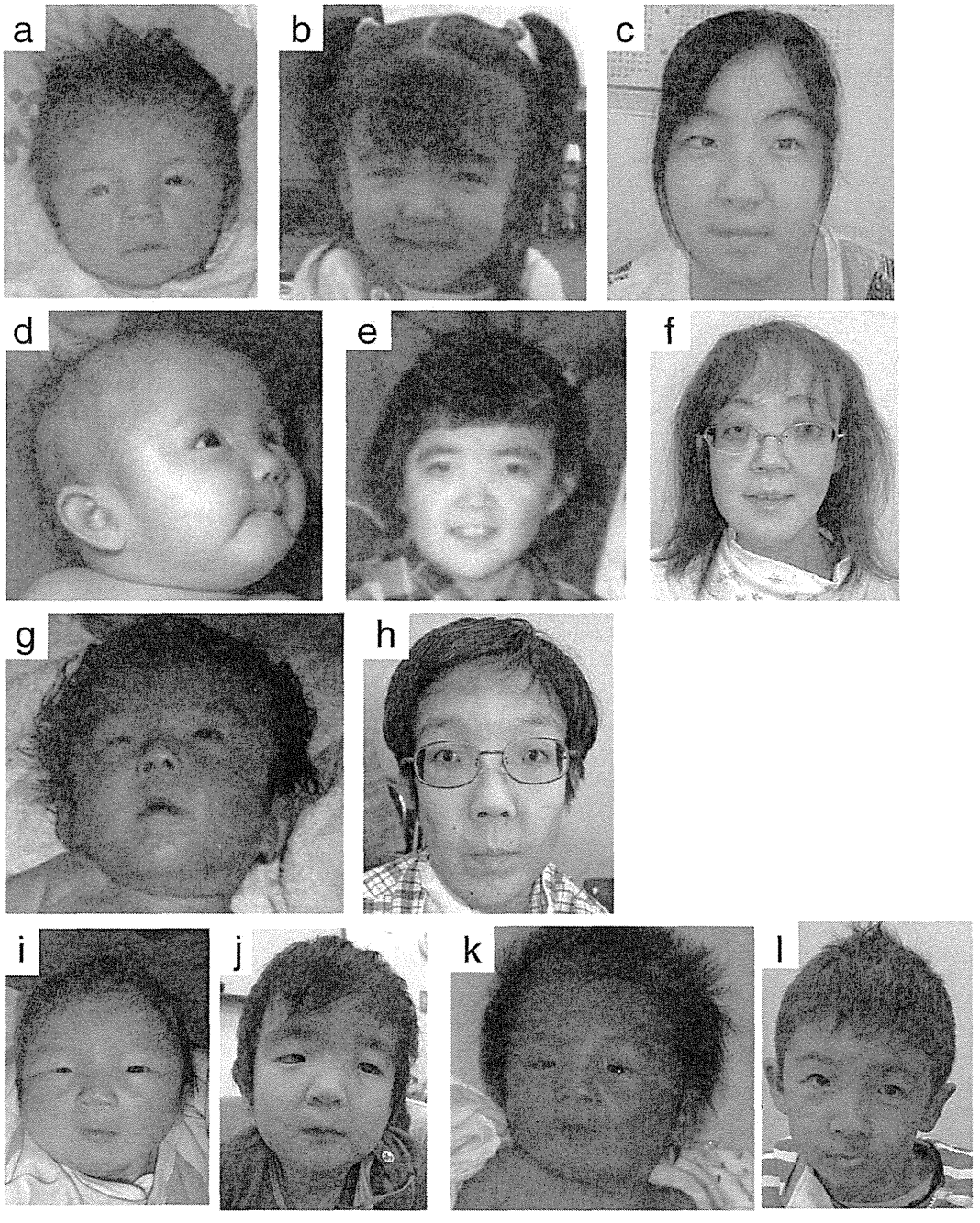

Fig. 1 Craniofacial features of patients with EDS caused by CHST14/D4ST1 deficiency. Patient 12 at age (a) 23 days, (b) 3 years, and (c) 16 years. Patient 13 at age (d) 3 months, (e) 5 years, and (f) 28 years. Patient 14 (g) in the neonatal period and (h) at age 28 years. Patient 21 (i) at age 15 days and (j) 2 years and 10 months. Patient 22 (k) at birth and (l) age 6 years and 6 months. Patient number is according to Table 2. (a–h, reproduced from Kosho et al. Am. J. Med. Genet. Part A. 2010; 152A: 1333–46, with permission from Wiley-Liss, Inc.; i–l, reproduced from Shimizu et al. Am. J. Med. Genet. Part A. 2011; 155A: 1949–58, with permission from Wiley-Liss, Inc.)

Gastrointestinal features

Constipation has been frequently recorded. Two adult patients developed diverticula perforation, which was corrected surgically.[6] One adolescent patient developed a severe progressive gastric ulcer that was treated with partial gastrectomy.[6] Other complications associated with gastrointestinal malformations include a common mesentery, spontaneous volvulus of the small intestine associated with absent gastrocolic omentum, and duodenal obstruction due to malrotation.[12]

Genitourinary features

Hydronephrosis was detected in six patients. The hydronephrosis was caused by renal ptosis in one patient, who underwent laparoscopic placement of a ureteral stent, but this procedure was

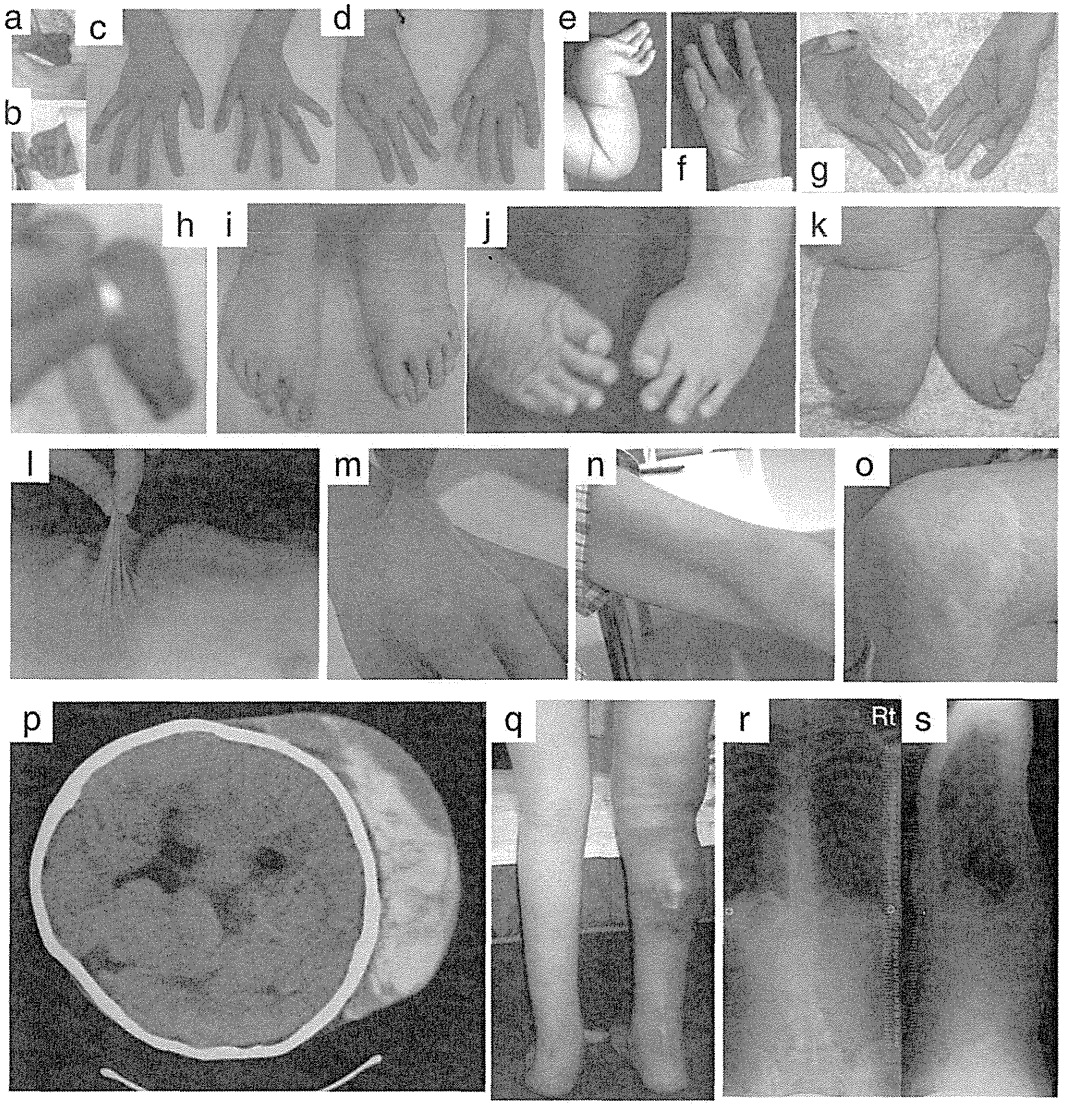

Fig. 2 Other physical features of patients with EDS caused by CHST14/D4ST1 deficiency. Patient 12 at (h) birth, (a, b) age 23 days, (p) 6 years, and (c,d,i,r,s) 16 years. Patient 13 at age (j) 2 months, (e) 3 months, (l) 1 year and 2 months, (f) 5 years, and (g,k) 28 years. (n,o) Patient 14 at age 30 years. Patient 16 at age (q) 16 years and (m) 19 years. Patient number is according to Table 2. (f,l,p, reproduced from Kosho et al. Am J. Med. Genet. Part A. 2005; 138A: 282–7, with permission from Wiley-Liss, Inc; a–e,g–k,m–o,q–s, reproduced from Kosho et al. Am. J. Med. Genet. Part A. 2010; 152A: 1333–46, with permission from Wiley-Liss, Inc.)

complicated by severe hemorrhage due to tissue fragility.[8] Another patient had a pelviureteric junction obstruction requiring nephrostomy in the neonatal period.[20] Nephrolithiasis or cystolithiasis was observed in five patients. Cryptorchidism was observed in most male patients. One patient who underwent orchidopexy developed hypogonadism in adulthood.[6] Poor breast development was noted in six female patients beyond adolescence.

Ophthalmological features

Refractive errors, typically myopia followed by astigmatism and hypermetropia, were described in 14 patients; strabismus in 12 patients; microcornea in seven; glaucoma or elevated intraocular pressure in six; and retinal detachment in five.

Otological features

Hearing impairment has been described in eight patients (specified for high-pitched sounds in four).

Neurological features

Ventricular enlargement/asymmetry has been described in eight patients on brain ultrasonography, computed tomography, or magnetic resonance imaging. Additional minor findings were also recorded: absence of the left septum pellucidum;[12] short corpus callosum with lack of an isthmus and well-defined rostrum, mild prominence of the Sylvian fissures, and a few small gray matter heterotopias along the lateral walls of the temporal horns of the lateral ventricles;[17] absence of the septum pellucidum, hypoplasia of the inferior vermis with a normally sized posterior fossa

(Dandy–Walker variant), hypoplasia of the hippocampi and splenium of the corpus callosum, and hypoplasia of the optic nerves (septo-optic dysplasia);[19] and mild cerebellar hypoplasia, hypoplasia of the cerebellar vermis (reminiscent of Dandy–Walker variant), and absence of the septum pellucidum.[20] Spinal cord tethering was noted in three patients,[6,12,19] two of whom underwent corrective surgery.

Growth features

Mild prenatal growth restriction has been suggested: mean birth length –0.5 SD and median –0.6 SD (n=9; range, –1.6 to +1.3 SD); mean birthweight –0.6 SD and median –0.67 SD (n=11; range, –2.0 to +0.5 SD); and mean birth occipital frontal circumference –0.2 SD and median –0.5 SD (n=8; range, –1.0 to +1.0 SD).[16] Mild postnatal growth restriction has also been suggested with slenderness and relative macrocephaly: mean height, –0.9 SD and median –0.6 SD (14 data points from 12 patients; range, –3.9 to +1.2 SD); mean weight –1.5 SD and median –1.4 SD (11 data points from nine patients; range, –2.4 to –0.4 SD); and mean occipital frontal circumference –0.2 SD and median 0.0 SD (10 data points from eight patients; range, –1.2 to >2.0 SD).[16]

Development

Gross motor developmental delay was described in 18 patients mainly because of muscle hypotonia. The median age at which unassisted walking occurred in patients who accomplished it was 2 years 1 month (n=8; range, 1 year 5 months–4 years).[16] One adult patient could not walk unassisted because of severe foot deformities (Fig. 2k) and leg muscle weakness.

A myopathic process was suggested as the cause of the muscle weakness in a patient with muscle action potentials with reduced amplitude but normal distal latency and nerve conduction velocity on electromyography; muscle biopsy showed no histological abnormalities.[9] In another patient, quantitative muscle ultrasonography showed increased echo intensity in the forearm extensors and anterior tibial muscles as well as marked bilateral atrophy of the forearm flexors, forearm extensors, and quadriceps. Nerve conduction studies showed low compound muscle action potential amplitudes in the distal muscles. Needle electromyography showed an abnormal and mixed pattern of short-duration, low-amplitude, polyphasic motor units, as well as polyphasic motor units with a longer duration and higher amplitude, reflecting an increase in fiber size diameter. Muscle biopsy showed fiber type 1 predominance without fiber type grouping, increased variation in the diameter of both type 1 and type 2 fibers, and some type 1 fibers in close proximity to lobulated fibers. These findings were compatible with a myopathy, similar to other EDS types.[18]

Mild intellectual delay was suggested in four patients; one reportedly had global psychomotor delay in infancy, but his IQ was around 90 at the age of 7 years 2 months.[9,12]

Etiology

Molecular abnormalities

Carbohydrate sulfotransferase 14, localized at 15q14, is a single-exon gene with an open reading frame of 1131 bp.[21] Mutations have been detected throughout the gene: R29Gfs*113 in one patient, V49X in three, K69X in one, Q113Rfs*14 in one, R135G in one, L137Q in one, F209S in one, R213P in one, R218S in one, G228Lfs*13 in one, R274P in one, M280L in one, P281L in eight, C289S in one, Y293C in four, and E334Gfs*X107 in one (Table 2; Fig. 3).[22,23] The sulfotransferase activity of cos-7 cells transfected with *CHST14* containing K69X, P281L, C289S, or Y293C mutations were decreased at almost the same level, suggesting that loss-of-function mutations in *CHST14* (i.e., CHST14/D4ST1 deficiency) are the basis of this disorder.[7]

Biochemical abnormalities

Glycosaminoglycans (GAG) such as dermatan sulfate (DS), chondroitin sulfate (CS), and heparan sulfate are side chains composed of repeating disaccharides bound to core proteins to form proteoglycans (PG).[23] Biosynthesis of CS and DS is shown in Figure 4. Human CHST14/D4ST1, comprising 376 amino acids and with an estimated molecular mass of 43 kDa, is a type II membrane protein with an N-terminal transmembrane region, binding sites for 3′-phosphoadenosine-5′-phosphosulfonate, and two potential *N*-glycosylation sites.[21] Evers *et al.* first cloned cDNA of *CHST14* based on its homology to *CHST10*, which codes for human natural killer-1 sulfotransferase.[21] They showed mRNA of *CHST14* to be expressed ubiquitously and the protein to transfer sulfate to the C-4 hydroxyl of *N*-acetyl-D-galactosamine (GalNAc) in the sequence L-iduronic acid (IdoA)-GalNAc immediately after epimerization of D-glucuronic acid (GlcA) to IdoA by DS epimerase, and designated the enzyme D4ST1.[21] Mikami *et al.* independently identified CHST14/D4ST1 by a public database search and further characterized its enzyme specificities, showing that partially desulfated DS also served as an excellent acceptor, while nearly completely desulfated DS had been reported to serve as an acceptor.[24]

Sulfotransferase activity toward dermatan in affected skin fibroblasts was significantly decreased to 6.7% in a patient with the compound heterozygous mutation P281L/Y293C (patient 12;

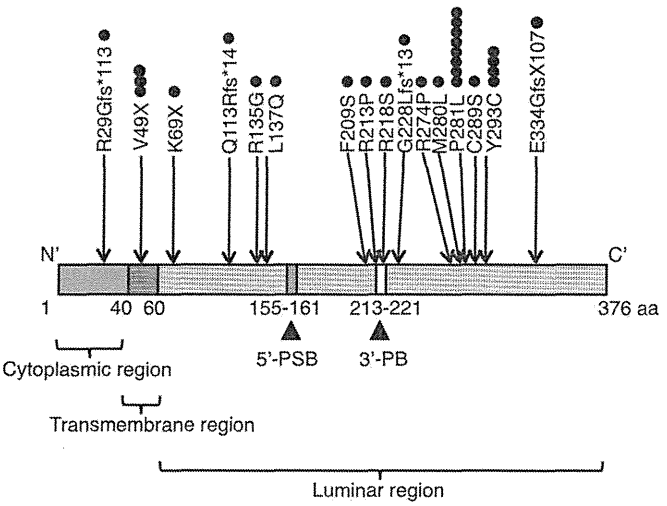

Fig. 3 Schematic representation of CHST14/D4ST1. All previously described patients (•) and mutations (arrows) are shown. 5′-PSB, 5′-phosphosulfate binding site; 3′-PB, 3′-phosphate biding site. (Reproduced from Kosho. Shinshu Med. J. 2011; 59: 305–19, with permission from Shinshu Medical Society.)